Journal of Integrative Agriculture 2026, 25(9): 3548–3558

Available online at ScienceDirect

Journal of Integrative Agriculture

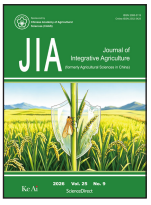

RESEARCH ARTICLE

Genetic identification and characterization of a novel locus for wheat kernel length

Qian Liu[1*], Qijing Xuan[1*], Yuxin Lan[1], Xinlin Xie[1], Bin Chen[1], Jianing You[2], Longxing Su[1], Md Nahibuzzaman Lohani[1], Lei Wu[1], Xinrong Hu[1], Li Yin[1], Yanlin Liu[1], Tongzhu Wang[1], Qiantao Jiang[1], Yuming Wei[1], Youliang Zheng[1], Chunji Liu[3], Hongwei Geng[4#], Jian Ma[1#]

[1] *State Key Laboratory of Crop Gene Exploration and Utilization in Southwest China/Triticeae Research Institute, Sichuan Agricultural University, Chengdu 611130, China*

[2] *Industrial Crop Research Institute, Sichuan Academy of Agricultural Sciences, Chengdu 610300, China*

[3] *School of Agriculture, Henan Institute of Science and Technology, Xinxiang 453003, China*

[4] *College of Agronomy/High Quality Special Wheat Crop Engineering Technology Research Center, Xinjiang Agricultural University, Urumqi 830052, China*

Highlights

- A novel locus for kernel length was identified and validated.
- A new model for analyzing the genetic basis of quantitative traits was proposed.

Abstract

Kernel length (KL) is one of the components that determine grain weight (GW) in wheat. In this study, a putative locus on chromosome arm 2BL was identified from mutant BLS2 with long kernels using a bulked segregant analysis (BSA) combined with a 60K SNP array. This putative locus was then confirmed as a major and stable QTL based on linkage mapping. The locus, *Qkl.sau-BC-2B.1*, was mapped in an interval of 0.4 cM, and the phenotypic variance explained by it varied from 17.01 to 30.53% across different environments. The effects of this locus were further verified in a second population. The positive allele of the locus could significantly increase hundred-kernel weight and prolong the anthesis date, but it did not affect plant height, tiller number, spike length, or spikelet number per spike. Expression and sequencing analyses identified *TraesCS2B02G478100*, which has a G to C transition variation leading to an amino acid change, as the likely candidate gene underlying this locus. In addition, a new model for analyzing the genetic basis of yield-related traits is proposed. Taken together, our results provide a foundation for subsequent gene mining and the use of this promising QTL in breeding for KL.

Keywords: wheat, kernel length, BSA, 60K SNP array, QTL mapping

1. Introduction

Wheat (*Triticum aestivum* L.) is one of the world's most important food crops, since it serves as the staple food for 30% of the global population (Li *et al.* 2021). Wheat yield is determined by three main factors: spike number per unit area, kernel number per spike, and thousand-kernel weight (TKW) (Hou *et al.* 2017). Assuming stability in kernel number per spike and spike number per unit area, changes in TKW significantly influence wheat yield. Kernel length (KL), kernel thickness (KT), and kernel width (KW) are highly correlated with TKW and directly impact both the yield and quality of wheat (Gegas *et al.* 2010; Okamoto *et al.* 2013). Enhancing these kernel traits is an effective strategy for increasing the crop yield. KL is a crucial factor affecting kernel size, so it indirectly influences grain weight (GW) and, consequently, yield. Larger kernels are directly linked to higher kernel yield and also positively affect seed vigor and the growth of wheat seedlings (Sun *et al.* 2017). Thus, the genetic enhancement

Received 4 September 2024; Received in revised form 24 September 2024; Accepted 25 September 2024; Available online 26 October 2024
[#]Correspondence Jian Ma, E-mail: jianma@sicau.edu.cn; Hongwei Geng, E-mail: hw-geng@163.com
[*] These authors contributed equally to this study.

doi: 10.1016/j.jia.2024.10.005

of wheat kernel traits is essential for developing high-yield and high-quality wheat varieties.

A quantitative trait locus (QTL) is a genomic region where genes controlling quantitative traits are located (Alberts and Schughart 2010). Numerous QTLs associated with KL have been identified on almost all 21 wheat chromosomes (Zhou *et al.* 2021). For example, five KL-related QTLs were discovered on chromosomes 2B, 2D, and 7D, and the phenotypic variance accounted by them varied from 9.685 to 19.618% (Xin *et al.* 2020). Kumar *et al.* (2016) identified four major QTLs for KL on chromosomes 3A, 4B, 5B, and 7A using a population of recombinant inbred lines (RILs) derived from a cross between ND705 and PI414566 (WCB462). Using 185 RILs from a mapping population of Rye Selection 111/Chinese Spring, Ramya *et al.* (2010) identified six QTLs related to KL. These loci were located on six chromosomes: 1A, 2B, 2D, 5A, 5B, and 5D. Using three RIL populations, Cui *et al.* (2014) detected 13 QTLs related to kernel length. These loci were located on 10 chromosomes: 1B, 2A, 2B, 2D, 3A, 3B, 5A, 6B, 7A, and 7B. By analyzing a RIL population constructed from 20828 and SY95-71, Qu *et al.* (2021) identified a major QTL for KL on chromosome 1B. The phenotypic variance explained by that locus varied from 9.48 to 25.23%. They also identified a KL locus on chromosome 2D, *Qkl.sicau-SSY-2D*, based on a RIL population constructed from S849-8 and SY95-71 (Qu *et al.* 2022). However, wheat KL is a complex quantitative trait that is governed by multiple genes and sensitive to environmental factors (Breseghello and Sorrells 2007; Xie *et al.* 2022). Mining and developing new, superior germplasm resources are vital for yield improvement and wheat breeding.

In this study, a RIL population consisting of 126 lines was developed from a cross between BLS2 (a mutant with long kernels) and cultivar 'Chuannong 16' (CN16). A 60K SNP array was employed in conjunction with bulked segregant analysis (BSA) to identify the chromosomal region controlling KL. Subsequently, KASP markers adjacent to these regions were developed and used to locate a QTL that controls wheat KL based on multi-year phenotypic data across various environments. The effect of this locus was then evaluated. Finally, candidate genes for the identified QTL were predicted.

2. Materials and methods

2.1. Plant materials

The mapping population used in this study, referred to as the BC population, contained 126 F_6 RILs produced by crossing BLS2 and CN16. The verification population, denoted as the BS population, consisted of 202 F_4 lines produced from a cross between BLS2 and SY95-71. BLS2 is an EMS-induced mutant from the genotype LJ2135, which is a genetically stable line derived from crossing a spelt wheat (*Triticum spelta* L., LS5893) and a common wheat (JM6893). This mutant possesses the characteristic of long kernel lengths. Given its relatively better agronomic traits, including appropriate plant height and large spikes, LJ2135 was chosen as a breeding parent (Xie *et al.* 2022). Under conventional cultivation conditions, the KL of BLS2 can reach 8 mm, which is significantly longer than the KL of most wheat varieties selected in Sichuan, China (Li 2016). The genotypes CN16 and SY95-71 exhibit shorter kernel lengths than BLS2 and both have multiple tillers (Liu *et al.* 2018, 2020). CN16 (Chuanyu 12/87-429) boasts advantages such as a good plant architecture (Zheng *et al.* 2002; Liu *et al.* 2018), while SY95-71 is recognized for its excellent plant type and well-developed root system (Chen *et al.* 2022). BLS2 was obtained from Prof. Ahsan Habib at Khulna University, Bangladesh. CN16 and SY95-71 were from the Triticeae Research Institute of Sichuan Agricultural University, China.

2.2. Field trials and phenotypic evaluation

The mapping population of BC was planted in Wenjiang, Sichuan Province, China (103°51′E, 30°43′N) from 2019 to 2023 and in Chongzhou, Sichuan Province (103°38′E, 30°32′N) from 2021 to 2022. The validation population of BS was planted in Chongzhou in 2019 and 2020. Fifteen seeds were planted in each line, with a spacing of 0.1 m between seeds and 0.3 m between rows. Field management adhered to local standard practices (Zhao *et al.* 2023). To minimize marginal effects, eight individual plants in the middle of each row were selected for data collection. After natural air-drying, 30 seeds from each line were randomly selected and scanned using an Epson Expression 10000 XL color image scanner (Seiko Epson Corporation, Japan). The WinSEEDLE software (Regent Instruments Canada, Inc.) was used to analyze the scanned images and calculate KL and KW. The hundred-kernel weight (HKW) was determined by weighing 100 kernels from each line with an electronic balance. The anthesis date (AD) was recorded from the date of sowing to the date when more than half of the plants had flowered. Plant height (PH) was measured from the ground surface to the top of the main spike (excluding awns) at maturity. Fertile tillers was taken as the effective tiller number (ETN). Spike length (SL) was measured from the base to the top of the main spike (excluding awns), and spikelet number per spike (SNS) was calculated by counting the number of spikelets on the main culm spike of each plant. Details on the specific trait identification and planting conditions of the related materials are provided in Appendix A.

2.3. Statistical analysis

The broad-sense heritability (H^2) and the best linear unbiased prediction (BLUP) were calculated using SAS V8.0 (SAS Institute, Cary, NC, USA). Student's *t*-test and effect analyses were conducted using SPSS 27 (IBM SPSS, Armonk, NY, USA). The BLUP values of each phenotypic measurement in different environments were used for a correlation analysis. Excel and Origin 2022 were employed to create the frequency distribution maps and other associated charts.

2.4. Examination of kernel epidermal cells

The full and mature kernels of BLS2 and CN16 were obtained, and the length and width of their epidermal cells were examined and measured according to the manual of a scanning electron microscope (Quanta 450 FEG, FEI, Waltham, MA, USA). The kernels of the parents were fixed in FAA (formalin, acetic acid, 70% alcohol) and stored

in a refrigerator at 4°C for over 24 hours, after which the samples were sent to Chengdu Otron Biological Company, China for paraffin transverse sectioning. Upon the return of the samples, epidermal cells of the kernel sections were examined and scanned using a stereo microscope (SZX7, Olympus, Japan) and a fluorescence microscope (BX63, Olympus, Japan). Areas of equivalent size were selected using the Case Viewer, and the numbers and sizes of the cells were quantified using ImageJ software.

2.5. BSA-60K SNP analyses and KASP marker development

KL data from four environments was used to select lines with extreme KL, and two mixed pools of the lines were constructed for a 60K SNP array analysis. Initially, 30 lines with the longest KL and 30 lines with the shortest KL were chosen from each environment and sorted in descending order according to KL. Subsequently, the average KL across all environments was also sorted in descending order, and the top 30 and bottom 30 lines were selected. The intersection of these two sets of results was used to create the extreme long kernel pool and the extreme short kernel pool. BLS2 was included in the extreme long kernel pool, while CN16 was included in the extreme short kernel pool for BSA. Seeds from the pools were germinated, and leaf samples from the seedling stage were sent to Tcuni Technologies, Chengdu, China, for 60K SNP data collection. The differential SNP locations between the two extreme pools were statistically analyzed. The chromosome with the largest number of differential SNPs was designated as the target chromosome, and the density of differential SNPs along this chromosome was assessed to identify the region with the most densely located SNPs, which may correspond to the candidate gene region (Magwene *et al.* 2011). Subsequently, KASP markers were designed based on the differing SNPs within the candidate region, following the methods outlined in the KASP primer design manual (Ertiro *et al.* 2015). The synthesis of KASP primers was performed by Bioengineering (Shanghai) Co., China. Details of the KASP primers used in this experiment are presented in Appendix B. The specificity of the KASP markers was evaluated in the two parental lines. Finally, 126 lines of the BC population were genotyped using polymorphic markers.

2.6. Genotyping and genetic map construction

The CTAB method was used to extract genomic DNA (Stein *et al.* 2001). KASP markers, developed based on the results from the 60K SNP pool, were used to genotype the parental lines BLS2 and CN16. In addition, polymorphic markers were employed for genotyping the BC population. In this study, the total KASP reaction system volume was 10 μL, comprising 5 μL of 2xMaster Mix V1 (HC Scientific, Chengdu, China), 1.4 μL of mixed primers, 2.6 μL of ddH_2O, and 1 μL of DNA. The KASP reaction protocol was as follows: initial denaturation at 94°C for 15 min, followed by denaturation at 94°C for 20 s, and annealing at 60°C for 1 min for a total of 10 cycles (with each cycle's temperature reduced by 0.6°C); then denaturation at 95°C for 20 s, and annealing at 55°C for 1 min, for a total of 25 cycles, and a final fluorescence scan at 37°C for 1 min to acquire the results. The reaction process was conducted on a real-time PCR system (BioRad®, CFX-96). Based on the outcomes of KASP genotyping, a genetic linkage map was constructed using the Kosambi mapping function in JoinMap v4.0.

2.7. QTL mapping and validation

The Inclusive Composite Interval Mapping (ICIM) method within IciMapping 4.2 was employed for QTL mapping (Li *et al.* 2008). The Bip method, which is suitable for biparental populations, was used to analyze the KL data from six different environments and the BLUP values. In addition, the multi-environmental trials (Met) functional module was used to detect interactions between environments and QTLs (Li *et al.* 2015). The parameters used for QTL analysis were as follows: PIN=0.001, Step=1 cM, and LOD=2.5 (Xie *et al.* 2022). In this study, QTLs detected in more than two different environments with an phenotypic variance explained (PVE) of over 10% were considered stable and major loci (Ma *et al.* 2019; You *et al.* 2021).

According to the results of QTL mapping, the KASP marker *K_sau_2B_683365530*, which is closely linked to *Qkl.sau-BC-2B.1*, was used to determine the effect of the locus in the validation population BS. A total of 138 lines from the BS population were selected for genotyping, and the KL values of different genotypes were statistically analyzed to evaluate the effect of the major locus on KL.

2.8. Candidate gene analysis

Flanking marker sequences of the major QTL mapped in this study were anchored to the corresponding chromosomes of Chinese Spring (IWGSC RefSeq v2.1) and wild emmer (*T. turgidum* ssp. *dicoccoides*, WEWSeq v2.0) (Ma *et al.* 2021; Xie *et al.* 2022), allowing for the identification of possible candidate genes. The results of previous studies were summarized and the QTL of KL along with the physical location information of related genes were retrieved from NCBI (https://www.ncbi.nlm.nih.gov/) and GrainGenes (https://wheat.pw.usda.gov/GG3/). These data were then compared with the major QTL identified in this study to reveal their potential relationships.

2.9. Expression analysis of candidate genes

The expression patterns of genes within the *Qkl.sau-BC-2B.1* interval were analyzed on WheatOmics 1.0 (http://202.194.139.32/expression/wheat.html), and potential candidate genes were identified in conjunction with previous studies. Samples of developing kernels and glumes were collected at 5, 10, and 15 days after flowering for total RNA extraction, with three biological replicates per time point. Total RNA was extracted using the Plant RNA Extraction Kit V1.5 (Biofit, Chengdu, China). Complementary DNA (cDNA) was synthesized using the ABScript Neo RT Master Mix for qPCR with gDNA remover (RK20433) (ABclonal, Wuhan, China). The RT-qPCR reaction system (10 μL) contained 1 μL cDNA, 5 μL ChamQ Universal SYBR qPCR Master Mix, 0.2 μL forward primers, 0.2 μL reverse primers, and 3.6 μL RNase-free H_2O. The RT-qPCR reaction protocol was as follows: initial pre-denaturation at 95°C for 10 min; followed by denaturation at

95°C for 10 s, annealing at 60°C for 30 s, and extension at 72°C for 10 s, for a total of 35 cycles; finally, fluorescence was detected with each 0.5°C decrement from 95 to 65°C, and the melt curve information was collected. Employing *β-actin* as an internal reference gene, each sample was analyzed with three biological and three technical replicates. Gene transcription levels were calculated using the $2^{-\Delta\Delta Ct}$ method (Li *et al.* 2022), and the average value was determined.

2.10. Sequence analysis of candidate genes

The cDNA of BLS2 and CN16 was used as a template to amplify the coding sequences (CDS) of candidate genes, followed by cloning and sequencing. The reaction system for isolating the candidate gene CDS included 2 μL cDNA, 25 μL 2×Phanta Max buffer, 1 μL dNTP Mix (10 mmol L^{-1} each), 1 μL Phanta Max Super-Fidelity DNA polymerase, 17 μL ddH_2O, 2 μL reverse primers, and 2 μL forward primers. The PCR reaction protocol was as follows: initial denaturation at 95°C for 3 min, followed by 95°C for 15 s, 58°C–62°C for 15 s, 72°C (with 30–60 s per kilobase) for 35 cycles, a 5 min extension at 72°C, and a final hold at 12°C. The PCR products were visualized using a 1% agarose gel, and the target bands were excised, recovered, and purified using the DNA Purification Kit (TianGen, Beijing, China). Subsequently, the purified products were cloned into the pMD^{TM}19-T vector (TaKaRa, Dalian, China). Three positive clones from each amplification product were randomly selected and sent to Beijing Tsingke Biotechnology Co. for sequencing. After obtaining the CDS of the related genes from both parents, DNAMAN was employed to compare the sequence differences. Details of the gene amplification primers and qPCR primers used in this experiment are presented in Appendix C.

3. Results

3.1. Phenotypic evaluation

The overall morphology of the parents and some representative lines is depicted in Appendix D. In all environments, the KL of BLS2 was significantly higher than that of CN16, while the KW and HKW of BLS2 were significantly lower than those of CN16 (Fig. 1-A; Table 1). Paraffin sections revealed that the epidermal cells of BLS2 were 10.81% longer and 29.31% wider than those of CN16 (Fig. 1-B), a finding confirmed by scanning electron microscopy (Appendix E). The KL, KW, HKW, and corresponding BLUP values of the BC population exhibited normal distributions over multiple environments, indicating that they are quantitative traits controlled by multiple genes (Fig. 2). The ranges of KL, KW, and HKW in the BC population were 6.29–9.20 mm, 2.81–4.37 mm, and 3.18–6.76 g, respectively. The broad-sense heritability (H^2) of KL was 0.52, indicating that it is primarily influenced by genetic factors. The coefficient of variation (CV) for the same trait was similar across different environments, and the phenotypic data for the three kernel-related traits displayed clear transgressive segregation in all environments. This suggests that favorable alleles may be present in both parents and that recombination of these loci occurred in the offspring (Table 1).

3.2. Correlation and variance analysis

We analyzed the KL and KW across six environments and the HKW across four environments. KL, KW, and HKW exhibited significant positive correlations in most environments, with correlation coefficients ranging from 0.24 to 0.95. The exceptions included the 2020CZ and 2021CZ environments (P<0.01; Fig. 3). The correlation analysis among kernel traits revealed that KL, KW, and HKW were significantly and positively correlated, with correlation coefficients ranging from 0.24 to 0.71 (P<0.01; Table 2). The correlation analysis between kernel traits and other agronomic traits indicated that KL was positively correlated with PTN and AD, and the correlation coefficients were 0.22 and 0.20, respectively. KW showed a significant positive correlation with PH, with a correlation coefficient of 0.31. HKW was significantly and positively correlated with both PTN and PH, with correlation coefficients of 0.23 and 0.21, respectively (Table 3).

3.3. The chromosomal interval associated with KL

Based on the 60K SNP array analysis, polymorphic SNPs between the two pools were identified and mapped onto the 21 chromosomes of wheat. Statistical analysis revealed an increased enrichment of differential SNPs on chromosome 2B (669) (Fig. 4-A). Further analysis indicated that the

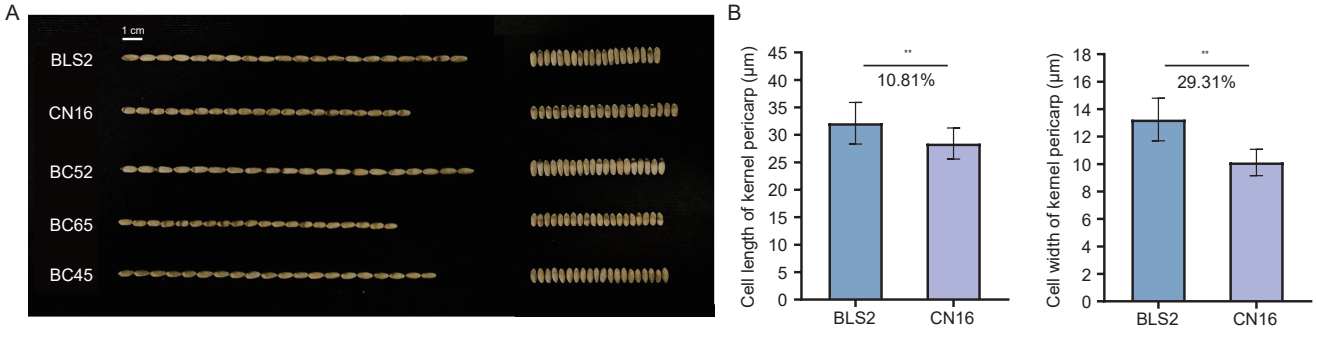

Fig. 1 Observations of kernel phenotypes of the parents (BLS2 and CN16) and some representative lines in the mapping population, and identification of the epidermal cell size in mature kernels of the parents (BLS2 and CN16). A, kernel phenotypes of the parents (BLS2 and CN16) and selected lines from the mapping population. B, comparison of the length and width of pericarp cells in paraffin sections of kernel transverse sections. Bars mean SD (BLS2, n=14; CN16, n=15). **, P<0.01.

differential SNPs were most enriched in the 620–700 Mb region of that chromosome (Fig. 4-B), suggesting this interval contains the locus that regulates KL.

3.4. Construction of the genetic map and QTL detection

Initially, 30 pairs of KASP markers within the 620–700 Mb interval on chromosome 2B were developed based on polymorphic SNPs, and 18 of them successfully differentiated the parents. Subsequently, a genetic map spanning 28.8 cM and containing 16 markers was constructed for the target interval. The remaining two polymorphic markers were not linked with the mapped markers (Fig. 4-C). *Qkl.sau-BC-2B.1* was mapped across four environments and a BLUP dataset with LOD scores ranging from 5.10 to 9.97 (Table 4), accounting for 17.01–30.53% of the phenotypic variance. The flanking markers of *Qkl.sau-BC-2B.1* were *K_sau_2B_682687604* and *K_sau_2B_683365530*, with a genetic distance of 0.40 cM.

Table 1 Phenotypic data for the parental and recombinant inbred line (RIL) populations in different environments

Trait[1)]	Environment[2)]	Parents		RIL					
		BLS2	CN16	Min	Max	Mean	SD	CV (%)	H^2
KL (mm)	2020CZ	8.58**	7.36	6.39	8.82	7.87	0.49	6.23	0.52
	2021CZ	8.40**	7.05	6.63	9.20	8.07	0.45	5.58	
	2022WJ	8.19**	6.91	6.29	8.93	7.37	0.40	5.43	
	2022CZ	8.10**	6.99	6.82	8.51	7.58	0.38	5.01	
	2023WJ	8.49**	7.20	6.80	8.65	7.60	0.35	4.61	
	2023CZ	8.50**	7.18	6.70	8.80	7.80	0.35	4.49	
	BLUP	8.30	7.19	6.97	8.50	7.72	0.28	3.63	
KW (mm)	2020CZ	3.72**	4.16	3.15	4.18	3.70	0.21	5.68	
	2021CZ	3.61**	4.09	3.11	4.27	3.79	0.21	5.54	
	2022WJ	3.34**	3.90	2.81	4.15	3.66	0.20	5.46	
	2022CZ	3.47**	3.72	3.18	4.37	3.77	0.19	5.04	
	2023WJ	3.41**	3.72	2.98	4.20	3.70	0.17	4.59	
	2023CZ	3.31**	3.72	3.12	4.18	3.68	0.16	4.35	
	BLUP	3.53	3.85	3.32	4.03	3.72	0.10	2.69	
HKW (g)	2022WJ	4.71**	5.08	3.79	6.76	5.19	0.54	10.40	
	2022CZ	4.62**	5.39	3.87	6.76	5.42	0.58	10.70	
	2023WJ	4.64**	4.84	3.18	6.45	4.75	0.54	11.36	
	2023CZ	4.47**	4.84	3.32	5.89	4.72	0.49	10.38	
	BLUP	4.67	5.04	3.87	5.88	5.02	0.39	7.77	

[1)] KL, kernel length; KW, kernel width; HKW, hundred-kernel weight.
[2)] WJ, Wenjiang; CZ, Chongzhou, Sichuan Province, China. BLUP, the best linear unbiased prediction.
** indicates the difference is significant at the 0.01 level.

3.5. Multi-environment analysis and effect assessment of *Qkl.sau-BC-2B.1*

The multi-environment QTL analysis revealed that the major locus *Qkl.sau-BC-2B.1* was detected in both single-environment and multi-environment QTL analyses (Appendix F). The LOD score in the multi-environment detection was 32.50, while that in the single-environment detection was 23.60, suggesting that the locus was stably expressed and not significantly influenced by environmental factors. The results from analyzing the impact of *Qkl.sau-BC-2B.1* in the BC population showed that lines possessing the *Qkl.sau-BC-2B.1* locus exhibited greater KL (Fig. 5-A).

3.6. Validation of the major QTL for KL

One of the flanking markers, *K_sau_2B_682687604*, was used to genotype the validation population BS, with the aim of further verifying the genetic effect and stability of *Qkl.sau-BC-2B.1*. The results from this analysis showed that in two environments (2020 CZ and 2021 CZ) and the BLUP of the BS population, the KL of lines sharing the same alleles as the parent BLS2 was significantly higher than that of lines with the same alleles from SY95-71 (P<0.01; Fig. 5-B), with increases of 4.42 to 5.90%. These findings further confirm that *Qkl.sau-BC-2B.1* is a stable QTL.

3.7. Genetic correlation between the major QTL and other traits of agronomic importance

The possible impacts of *Qkl.sau-BC-2B.1* on other traits of agronomic importance, including KW, HKW, PH, PTN,

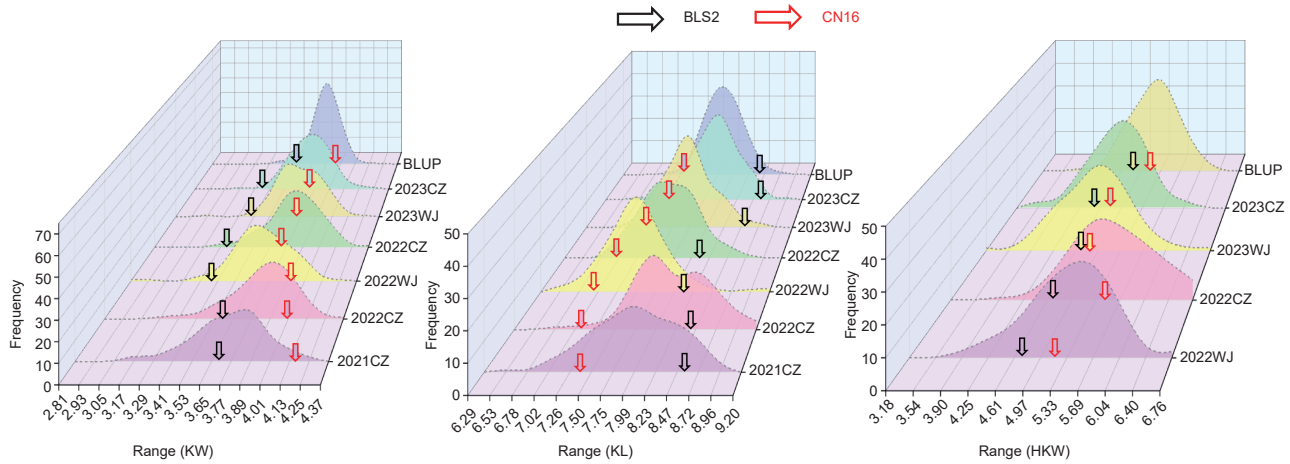

Fig. 2 Frequency distributions of kernel length, kernel width and hundred-kernel weight in different environments. WJ, Wenjiang; CZ, Chongzhou, Sichuan Province, China. BLUP, the best linear unbiased prediction. KW, kernel width; KL, kernel length; HKW, hundred-kernel weight.

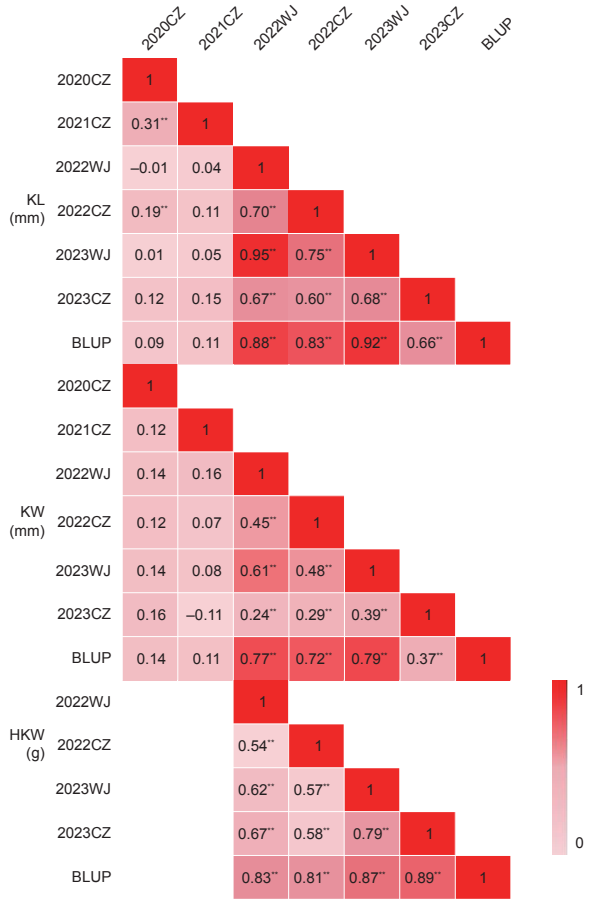

Fig. 3 Correlation coefficients of kernel characteristics in different environments. WJ, Wenjiang; CZ, Chongzhou, Sichuan Province, China. BLUP, the best linear unbiased prediction. KL, kernel length; KW, kernel width; HKW, hundred-kernel weight. **, significant at the 0.01 level.

Table 2 Correlation coefficients among different kernel characteristics in the mapping population BC[1)]

	KL	KW	HKW
KL	1		
KW	0.24**	1	
HKW	0.59**	0.71**	1

[1)] KL, kernel length; KW, kernel width; HKW, hundred-kernel weight.
** significant at the 0.01 level.

Table 3 Correlation coefficients among kernel characteristics and other traits of agronomic importance[1)]

	PTN-BLUP	PH-BLUP	SL-BLUP	SNS-BLUP	AD-BLUP
KL-BLUP	0.22**	–0.05	0.17	0.09	0.20**
KW-BLUP	0.14	0.31**	0.15	0.10	–0.06
HKW-BLUP	0.23**	0.21**	0.15	0.07	0.01

[1)] KL, kernel length; KW, kernel width; HKW, hundred-kernel weight. PTN, productive tiller number; PH, plant height; SL, spike length; SNS, spikelet number per spike; AD, anthesis date. BLUP, the best linear unbiased prediction.
**, significant at the 0.01 level.

SL, SNS, and AD, were assessed. This assessment found that lines possessing the positive allele at *Qkl.sau-BC-2B.1* exhibited a 6.79% increase in HKW and a 0.21% increase in AD. Significant differences were also noted in KW, PH, PTN, SL, and SNS between lines with positive and negative alleles of *Qkl.sau-BC-2B.1* (Fig. 6). Further, the constructed map was used to map a major and stably expressed locus for HKW, which revealed that the positive allele of HKW was also contributed by BLS2. It was located in the same interval as *Qkl.sau-BC-2B.1* (Appendix G).

3.8. Gene prediction within the interval of *Qkl.sau-BC-2B.1*

The two markers flanking the major QTL *Qkl.sau-BC-2B.1* had a physical distance of 0.68 Mb (from 682.69 to 683.37 Mb) based on the reference genome of CS. A BLAST search found 14 genes within that interval, including eight high-confidence genes and six low-confidence genes (Appendix H). Comparison with the genome of *T. spelta* L. revealed that the eight high-confidence genes were orthologous to those of *T. spelta* L. (Appendix I).

The annotation results indicated that four of these genes might be associated with the regulation of kernel development (Appendix H). A temporal and spatial expression analysis of these genes using public expression data showed that only *TraesCS2B02G478100* exhibited elevated expression in kernels (Appendix I). Subsequently, the CDS of *TraesCS2B02G478100* was isolated from both BLS2 and CN16. Comparative analysis revealed a SNP in the gene that differed between the parental lines BLS2 and CN16 (Fig. 7-A). The SNP was characterized by a G to C transition which led to an amino acid change at the 61st position from alanine to phenylalanine (Fig. 7-B). However, significant differences in the expression of *TraesCS2B02G478100* in kernels at 5, 10, and 15 days post-flowering were not detected between BLS2 and CN16 (Appendix J).

4. Discussion

4.1. Comparison of *Qkl.sau-BC-2B.1* with loci identified in previous studies

This study identified a major and stable QTL, *Qkl.sau-BC-2B.1*, controlling KL in wheat. This QTL was mapped to an interval of 682.69–683.37 Mb on 2BL based on the reference genome of Chinese Spring. In contrast, the QTLs related to KL previously mapped on chromosome 2B were not only well separated from *Qkl.sau-BC-2B.1* but also had only minor effects on KL (Appendix K). For example, Ma *et al.* (2017) mapped the orthologous gene *TaGW7* of *OsGW7* to the short arms of homoeologous group 2 chromosomes (2AS, 2BS, and 2DS) by homologous cloning, and the physical location for the locus on 2BS was in the interval of 182.01–182.02 Mb. Mohler *et al.* (2004) mapped the photoperiod-related gene *Ppd-B1* to chromosome 2BS based on an analysis of three populations. In addition, several kernel-related regulatory genes have been identified on 2B. They include *TaGW2B* which affects the weight and size of wheat kernels (Hong *et al.* 2014). Genes such as *TaSUS-2B* and *TaSTT3b-2B*, which regulate grain weight, are located far away from *Qkl.sau-BC-2B.1* (Jiang *et al.* 2011; Zhu *et al.* 2022). Therefore, *Qkl.sau-BC-2B.1* is likely a novel QTL.

4.2. Candidate genes underlying *Qkl.sau-BC-2B.1*

Within the physical interval of *Qkl.sau-BC-2B.1*, 14

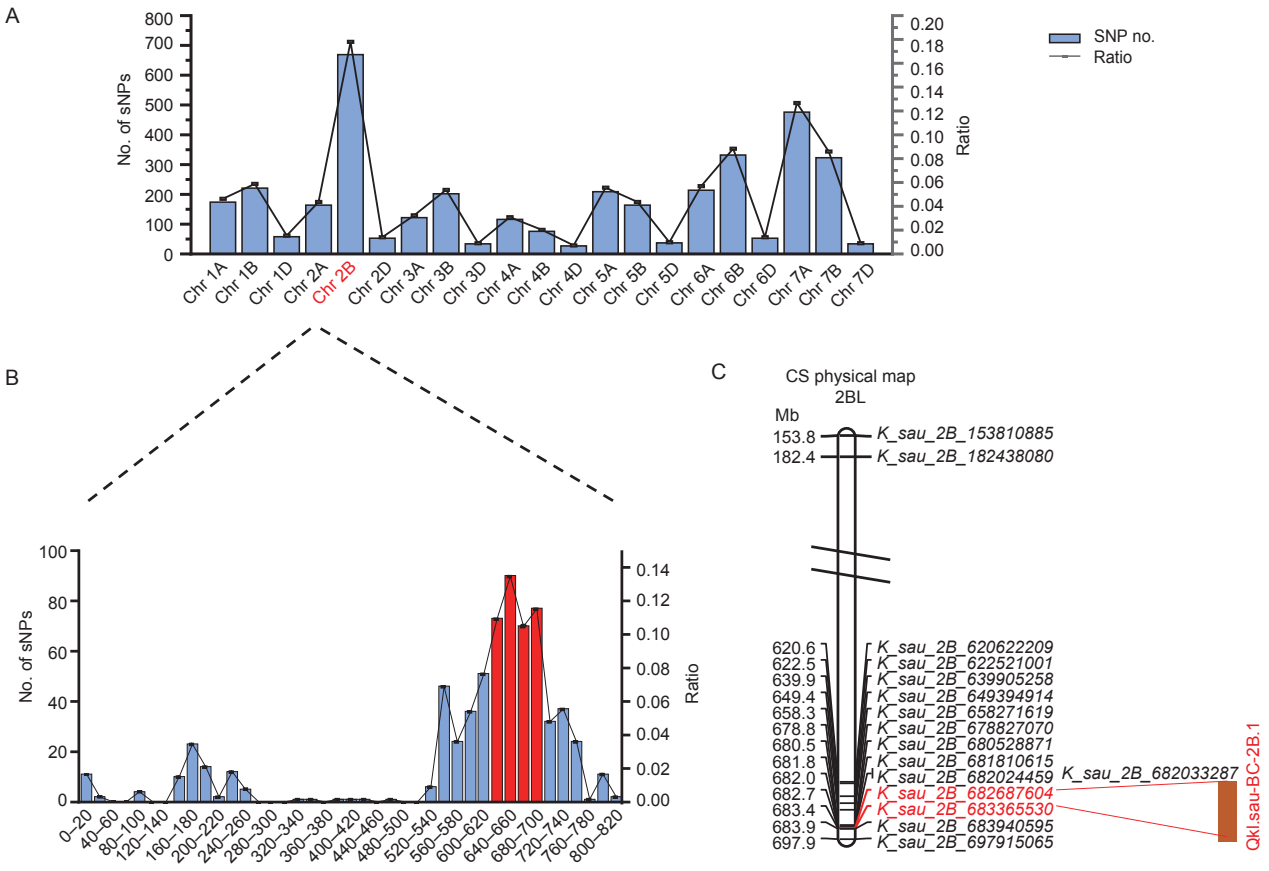

Fig. 4 BSA-60K SNP analysis and construction of the genetic maps. A and B, 60K SNP array-based analysis of SNPs. 'No. of SNPs' represents the number of homozygous polymorphic SNPs on each chromosome or segment; 'Ratio' represents the ratio of the number of homozygous polymorphic SNPs to the total SNPs. C, physical map of the major QTL (RefSeq v2.1).

Table 4 *Qkl.sau-BC-2B.1* for kernel length identified in the mapping population in different environments

Environment[1)]	Left marker	Right marker	LOD/PVE/Add[2)]
2022WJ	K_sau_2B_682687604	K_sau_2B_683365530	9.97/30.53%/0.18
2022CZ	K_sau_2B_682687604	K_sau_2B_683365530	5.10/17.01%/0.23
2023WJ	K_sau_2B_682687604	K_sau_2B_683365530	6.11/20.01%/0.18
2023CZ	K_sau_2B_682687604	K_sau_2B_683365530	5.17/17.34%/0.16
BLUP	K_sau_2B_682687604	K_sau_2B_683365530	5.49/18.45%/0.14

[1)] WJ, Wenjiang; CZ, Chongzhou, Sichuan Province, China. BLUP, the best linear unbiased prediction.
[2)] LOD, logarithmic odds; PVE, phenotype variation values; Add, additive effect of a QTL.

genes were found in the Chinese Spring reference genome. An analysis of these genes, including their expression patterns, annotations, and homology, indicated that *TraesCS2B02G477500*, *TraesCS2B02G477600*, *TraesCS2B02G477800*, and *TraesCS2B02G478100* may be associated with kernel development. Notably, *TraesCS2B02G477500* encodes a ring finger protein, a type known to play crucial roles in plant growth, stress resistance, photomorphogenesis, and signal transduction (Sun *et al.* 2019).

Meng *et al.* (2024) reported a gene (*TaSDIR1-4A*) encoding an E3 ligase-active innominate finger protein, which enhances the molecular mechanism of wheat drought resistance by mediating the ubiquitination and degradation of the membrane-bound transcription factor *TaWRKY29*. Wang *et al.* (2020) found that *TaSDIR1-4A* is a negative regulator of wheat kernel size. Yan *et al.* (2022) discovered that an unnamed finger protein, *OsPAGN1*, was highly correlated with rice kernel development. *TraesCS2B02G477600* encodes a lectin receptor kinase, which is known to play a significant role in stress responses during plant development (Bouwmeester and Govers 2009). Xiao *et al.* (2021) reported a lectin receptor-like kinase, *LecRK-VIII.2*. By coordinating seed size and seed number in *Arabidopsis*, this gene affects seed yield. *TraesCS2B02G477800* encodes a plant-specific protein, multiple chloroplast division site 1 (MCD1), which is essential for chloroplast division and may influence the accumulation of organic products (Nakanishi *et al.* 2009; Chen *et al.* 2018). *TraesCS2B02G478100* encodes a calcium-dependent protein kinase (CDPK/CPK), a key component

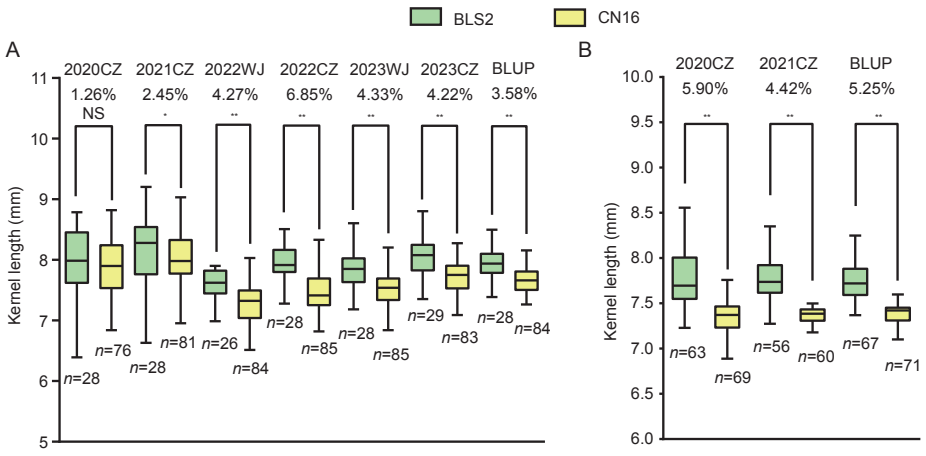

Fig. 5 Effect of the major QTL on kernel length in the BC population (A) and BS population (B). WJ, Wenjiang; CZ, Chongzhou, Sichuan Province, China; BLUP, the best linear unbiased prediction. Each boxplot incorporates maximum, minimum, median, lower quartile, and upper quartile. The rectangular box is framed by the two quartiles, whiskers connect the box to the extreme values, and the median is presented as a central line inside the box. *, $P<0.05$; **, $P<0.01$; NS, not significant.

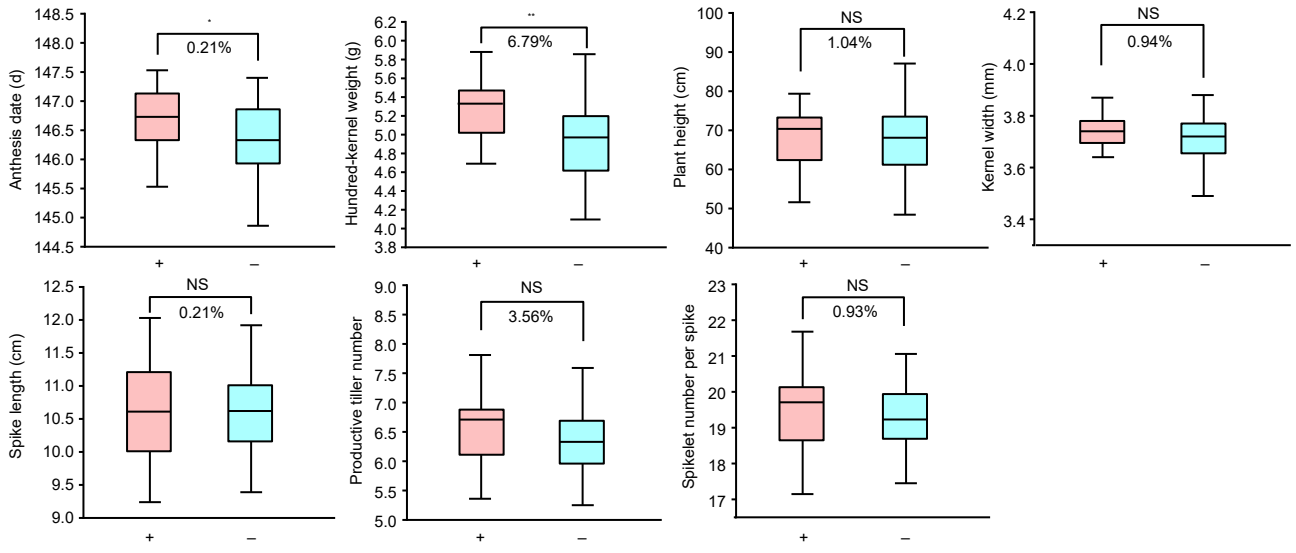

Fig. 6 Analysis of the effects of *Qkl.sau-BC-2B.1* on other traits of agronomic importance. + and – represent lines with and without *Qkl.sau-BC-2B.1*, respectively. Each boxplot incorporates maximum, minimum, median, lower quartile and upper quartile. The rectangular box is framed by the two quartiles, whiskers connect the box to the extreme values, and the median is presented as a central line inside the box. *, $P<0.05$; **, $P<0.01$; NS, not significant.

in signal transduction pathways. It is involved in bud and root development, pollen tube growth, stomatal movement, hormone signal transduction, transcription reprogramming, and stress tolerance in *Arabidopsis* (Delorme *et al.* 2019). Overexpression of *OsCPK19* was shown to seriously impair rice seed development, while *OsCPK31* regulates kernel development by affecting kernel filling (Morello *et al.* 2000; Manimaran *et al.* 2015). An analysis of the Chinese Spring expression database revealed that *TraesCS2B02G478100* exhibits high expression levels in the kernel. In this study, the CDS of the gene was isolated from the parental lines and a SNP variation between them was identified. These findings provide a foundation for the subsequent fine mapping of *Qkl.sau-BC-2B.1* and the cloning of the responsible gene(s).

4.3. Genetic correlations between kernel characteristics and other traits of agronomic importance

Consistent with previous studies, significant and positive correlations were detected among KL, KW, and HKW in this study. Further analysis of the potential effects of *Qkl.sau-BC-2B.1* on other traits of agronomic importance revealed that the positive allele of *Qkl.sau-BC-2B.1* significantly increased HKW and prolonged AD, but did not affect PH, ETN, SL, or SN. Results from previous studies showed that delayed anthesis often prolongs the development of young spikes, leading to longer spikes and more spikelets and is beneficial to yield improvement (Shaw *et al.* 2013). Although AD was also significantly prolonged in the data obtained in this study, the number of spikelets did not increase

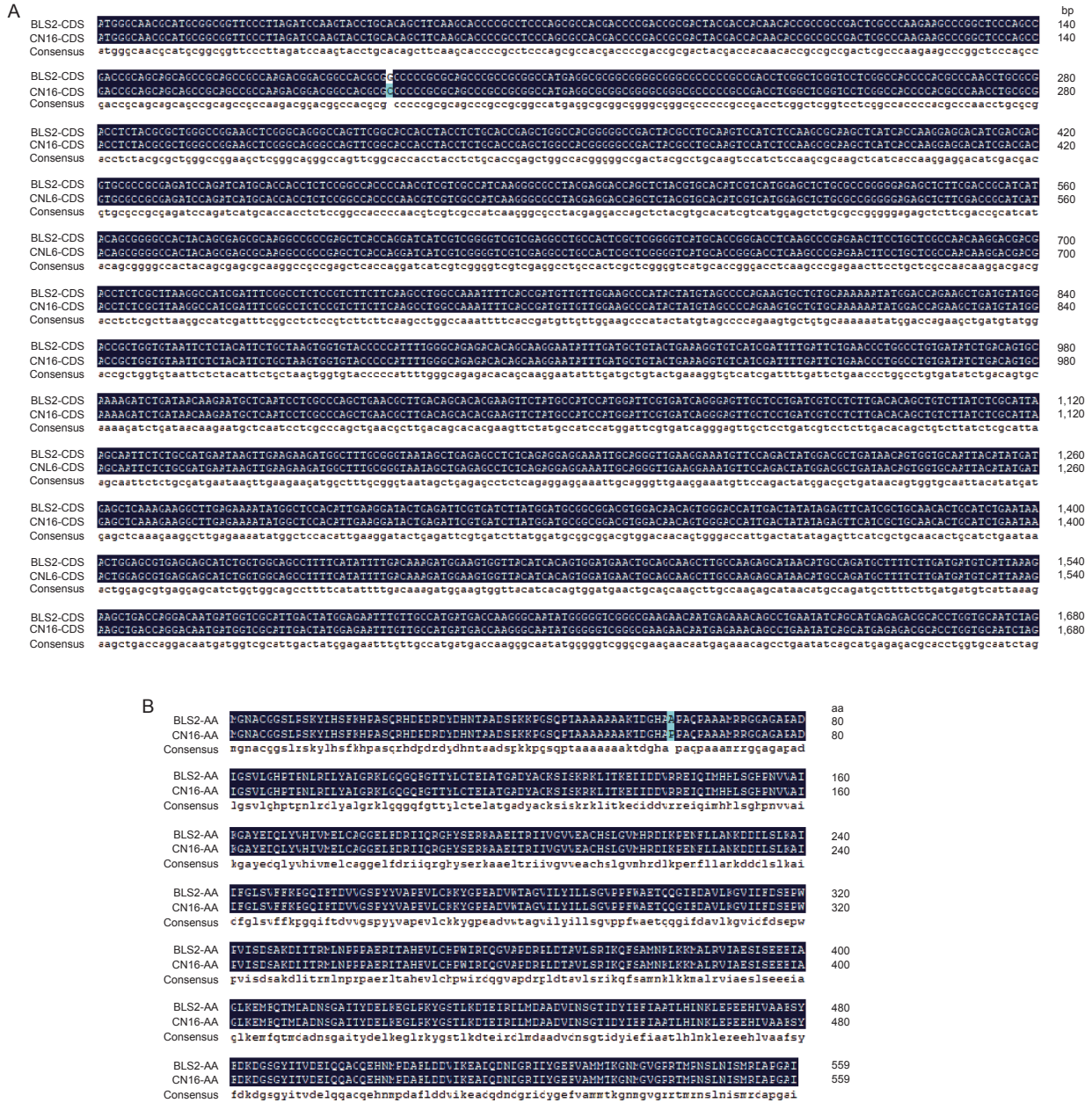

Fig. 7 Sequence analysis of *TraesCS2B02G478100* between the parents (BLS2 and CN16). A, coding sequence (CDS) alignment of *TraesCS2B02G478100* in the parents. B, amino acid sequence alignment of *TraesCS2B02G478100* in the parents.

significantly, suggesting that the genes regulating spikelet and flower development genes are likely to be independent. Lines containing the positive allele of *Qkl.sau-BC-2B.1* had greater KL and KW, indicating that this locus has great potential for high-yield breeding in wheat.

4.4. Application of a four-step method for analyzing the genetic basis of quantitative traits

In this study, a new model for analyzing the genetic basis of quantitative traits was proposed and implemented. This method was based on 'multiple environmental assessments, extreme phenotypic screening, mixed pool construction, and linkage map positioning' (referred to as the four-step method). This method was used to successfully locate the QTL conditioning KL in this study. A RIL population, constructed with BLS2 and CN16 as parents, was used to study KL across multiple environments. Lines with extreme KL from four environments between 2020 and 2022 were screened and used to construct mixed pools. In conjunction with the 60K SNP array, KASP primers were designed for genotyping, genetic linkage map construction, and the preliminary positioning of the KL loci. This approach not only ensured the accuracy of the mapping results but also significantly enhanced the efficiency of QTL mapping. The feasibility of the model described above has already been proven in our previous studies (Qu *et al.* 2022; Xie *et al.* 2022).

4.5. Feasibility of positioning loci based on BSA with the 60K SNP array

The method of combining BSA with SNP analysis has been widely used in studies on traits of agronomic importance in wheat. Based on such an approach, Kong *et al.* (2020) identified a wheat premature senescence gene, *Lmpa1*, on the short arm of chromosome 5A using an F_2 population of the cross LMPA1/Chinese Spring; Qu *et al.* (2022) located two major and stable QTLs affecting kernel length and grain weight on chromosome 2D; and Xin *et al.* (2020) located QTLs for kernel-related traits in wheat based on BSA+660K SNP array, validating the QTLs identified using QTL mapping analysis based on a genome-wide linkage map. These studies have demonstrated the feasibility of using BSA combined with an SNP array to locate genes for traits of agronomic importance in wheat. In this study, a genetic linkage map was constructed based on the results of BSA and a wheat 60K SNP array, and a major locus for KL was identified through phenotypic identification, further confirming the feasibility of BSA based on a 60K SNP array for genotyping and genetic mapping in wheat populations.

5. Conclusion

In this study, a novel major and stable QTL for KL, *Qkl.sau-BC-2B.1*, was detected and its candidate genes were identified. The genetic effects of that locus on major traits of agronomic importance were characterized using BSA combined with the 60K SNP array. This QTL could explain 17.01–30.53% of the phenotypic variance in different environments. Analyzing the Chinese Spring expression database revealed that *TraesCS2B02G478100* exhibits a high expression level in the kernel. Expression and sequencing analyses suggested that *TraesCS2B02G478100*, which has a G to C transition variation leading to an amino acid change between the two parental genotypes, is likely responsible for *Qkl.sau-BC-2B.1*. The results from this study provide a basis for subsequent gene cloning and breeding utilization.

Acknowledgements

This research was supported by the National Key R&D Program of China (2023YFD1201900), the Xinjiang Autonomous Region Major Science and Technology Special Project, China (2024A02003-2), the Xinjiang Agriculture Research System, China (XJARS-01-02), and the Natural Science Foundation of Sichuan Province, China (2024NSFSC0312). We thank the anonymous referees for their critical reading and revision of this manuscript.

Declaration of competing interest

The authors declare that they have no conflict of interest.

Declaration of generative AI and AI-assisted technologies in the writing process

The authors declare that they did not use AI in the preparation and writing of this manuscript.

Appendices associated with this paper are available at https://doi.org/10.1016/j.jia.2024.10.005

References

Alberts R, Schughart K. 2010. QTLminer: Identifying genes regulating quantitative traits. *BMC Bioinformatics*, **11**, 1–3.

Bouwmeester K, Govers F. 2009. *Arabidopsis* L-type lectin receptor kinases: Phylogeny, classification, and expression profiles. *Journal of Experimental Botany*, **60**, 4383–4396.

Breseghello F, Sorrells M E. 2007. QTL analysis of kernel size and shape in two hexaploid wheat mapping populations. *Field Crops Research*, **101**, 172–179.

Chen H, Wei J, Tian R, Zeng Z, Tang H, Liu Y, Xu Q, Deng M, Jiang Q, Chen G, Liu Y, Li W, Qi P, Jiang Y, Jiang Y, Tang L, Wei Y, Zheng Y, Lan X, Ma J. 2022. A major quantitative trait locus for wheat total root length associated with precipitation distribution. *Frontiers in Plant Science*, **13**, 995183.

Chen L, Sun B, Gao W, Zhang Q Y, Yuan H, Zhang M. 2018. MCD1 associates with FtsZ filaments *via* the membrane-tethering protein ARC6 to guide chloroplast division. *The Plant Cell*, **30**, 1807–1823.

Cui F, Zhao C, Ding A, Li J, Wang L, Li X, Bao Y, Li J, Wang H. 2014. Construction of an integrative linkage map and QTL mapping of grain yield-related traits using three related wheat RIL populations. *Theoretical and Applied Genetics*, **127**, 659–675.

Delormel T Y, Boudsocq M. 2019. Properties and functions of calcium-dependent protein kinases and their relatives in *Arabidopsis thaliana*. *New Phytologist*, **224**, 585–604.

Ertiro B T, Ogugo V, Worku M, Das B, Olsen M, Labuschagne M, Semagn K. 2015. Comparison of Kompetitive Allele Specific PCR (KASP) and genotyping by sequencing (GBS) for quality control analysis in maize. *BMC Genomics*, **16**, 908.

Gegas V C, Nazari A, Griffiths S, Simmonds J, Fish L, Orford S, Sayers L, Doonan J H, Snape J W. 2010. A genetic framework for grain size and shape variation in wheat. *The Plant Cell*, **22**, 1046–1056.

Hong Y, Chen L, Du L P, Su Z, Wang J, Ye X, Qi L, Zhang Z. 2014. Transcript suppression of *TaGW2* increased grain width and weight in bread wheat. *Functional & Integrative Genomics*, **14**, 341–349.

Hou J, Li T, Wang Y, Hao C, Liu H, Zhang X. 2017. ADP-glucose pyrophosphorylase genes, associated with kernel weight, underwent selection during wheat domestication and breeding. *Plant Biotechnology Journal*, **15**, 1533–1543.

Jiang Q, Hou J, Hao C, Wang L, Ge H, Dong Y, Zhang X. 2011. The wheat (*T. aestivum*) *sucrose synthase 2* gene (*TaSus2*) active in endosperm development is associated with yield traits. *Functional & Integrative Genomics*, **11**, 49–61.

Kong W, Wang L, Cao P, Li X, Ji J, Dong P, Yan X, Wang C, Wang H, Sun J. 2020. Identification and genetic analysis of EMS-mutagenized wheat mutants conferring lesion-mimic premature aging. *BMC Genetics*, **21**, 88.

Kumar A, Mantovani E, Seetan R, Soltani A, Echeverry-Solarte M, Jain S, Simsek S, Doehlert D, Alamri M, Elias E, Kianian S, Mergoum M. 2016. Dissection of genetic factors underlying wheat kernel shape and size in an elite × nonadapted cross using a high density SNP linkage map. *The Plant Genome*, **9**, 1–12.

Li C, Liu H, Wang J, Pan Q, Wang Y, Wu K, Jia P, Mu Y, Tang H, Xu Q, Jiang Q, Liu Y, Qi P, Zhang X, Huang L, Chen G, Wang J, Wei Y, Zheng Y, Gou L, *et al.* 2022. Characterization and fine mapping of a lesion mimic mutant (*Lm5*) with enhanced stripe rust and powdery mildew resistance in bread wheat (*Triticum aestivum* L.). *Theoretical and Applied Genetics*, **135**, 421–438.

Li H, Ribaut J M, Li Z, Wang J. 2008. Inclusive composite interval mapping (ICIM) for digenic epistasis of quantitative traits in biparental populations. *Theoretical and Applied Genetics*, **116**, 243–260.

Li J, Jiao G, Sun Y, Chen J, Zhong Y, Yan L, Jiang D, Ma Y, Xia L. 2021. Modification of starch composition, structure and properties through editing of *TaSBEIIa* in both winter and spring wheat varieties by CRISPR/Cas9. *Plant Biotechnology Journal*, **19**, 937–951.

Li S, Wang J, Zhang L. 2015. Inclusive composite interval mapping of QTL by environment interactions in biparental populations. *PLoS ONE*, **10**, e0132414.

Li Z. 2016. Agronomic traits evaluation and association analysis of wheat landraces in Southwest China. MSc thesis, Triticeae Research

Institute, Sichuan Agricultural University, China. (in Chinese)
Liu J, Luo W, Qin N, Ding P, Zhang H, Yang C, Mu Y, Tang H, Liu Y, Li W, Jiang Q, Chen G, Wei Y, Zheng Y, Liu C, Lan X, Ma J. 2018. A 55 K SNP array-based genetic map and its utilization in QTL mapping for productive tiller number in common wheat. *Theoretical and Applied Genetics*, **131**, 2439–2450.
Liu J, Tang H, Qu X, Liu H, Li C, Tu Y, Li S, Habib A, Mu Y, Dai S, Deng M, Jiang Q, Liu Y, Chen G, Wang J, Guangdeng C, Li W, Jiang Y, Wei Y, Lan X, *et al.* 2020. A novel, major, and validated QTL for the effective tiller number located on chromosome arm 1BL in bread wheat. *Plant Molecular Biology*, **104**, 173–185.
Ma J, Ding P, Liu J, Li T, Zou Y, Habib A, Mu Y, Tang H, Jiang Q, Liu Y, Chen G, Wang J, Deng M, Qi P, Li W, Pu Z, Zheng Y, Wei Y. 2019. Identification and validation of a major and stably expressed QTL for spikelet number per spike in bread wheat. *Theoretical and Applied Genetics*, **132**, 3155–3167.
Ma J, Ding P, Qin P, Liu Y, Xie Q, Chen G, Li W, Jiang Q, Chen G, Lan X, Wei Y, Liu C, Zheng Y. 2017. Structure and expression of the *TaGW7* in bread wheat (*Triticum aestivum* L.). *Plant Growth Regulation*, **82**, 281–291.
Ma S, Wang M, Wu J, Guo W, Chen Y, Li G, Wang Y, Shi W, Xia G, Fu D, Kang Z, Ni F. 2021. WheatOmics: A platform combining multiple omics data to accelerate functional genomics studies in wheat. *Molecular Plant*, **14**, 1965–1968.
Magwene P M, Willis J H, Kelly J K. 2011. The statistics of bulk segregant analysis using next generation sequencing. *PLoS Computational Biology*, **7**, e1002255.
Manimaran P, Mangrauthia S K, Sundaram R, Balachandran S. 2015. Constitutive expression and silencing of a novel seed specific calcium dependent protein kinase gene in rice reveals its role in grain filling. *Journal of Plant Physiology*, **174**, 41–48.
Meng Y, Lv Q, Li L, Wang B, Chen L, Yang W, Lei Y, Xie Y, Li X. 2024. E3 ubiquitin ligase *TaSDIR1*-4A activates membrane-bound transcription factor *TaWRKY29* to positively regulate drought resistance. *Plant Biotechnology Journal*, **22**, 987–1000.
Mohler V, Lukman R, Ortiz-Islas S, William M, Worland A J, Van Beem J, Wenzel G. 2004. Genetic and physical mapping of photoperiod insensitive gene *Ppd-B1* in common wheat. *Euphytica*, **138**, 33–40.
Morello L, Frattini M, Gianì S, Christou P, Breviario D. 2000. Overexpression of the calcium-dependent protein kinase *OsCDPK2* in transgenic rice is repressed by light in leaves and disrupts seed development. *Transgenic Research*, **9**, 453–462.
Nakanishi H, Suzuki K, Kabeya Y, Miyagishima S Y. 2009. Plant-specific protein MCD1 determines the site of chloroplast division in concert with bacteria-derived MinD. *Current Biology*, **19**, 151–156.
Okamoto Y, Nguyen A T, Yoshioka M, Iehisa J C, Takumi S. 2013. Identification of quantitative trait loci controlling grain size and shape in the D genome of synthetic hexaploid wheat lines. *Breeding Science*, **63**, 423–429.
Qu X, Li C, Liu H, Liu J, Luo W, Xu Q, Tang H, Mu Y, Deng M, Pu Z, Ma J, Jiang Q, Chen G, Qi P, Jiang Y, Wei Y, Zheng Y, Lan X, Ma J. 2022. Quick mapping and characterization of a co-located kernel length and thousand-kernel weight-related QTL in wheat. *Theoretical and Applied Genetics*, **135**, 2849–2860.
Qu X, Liu J, Xie X, Xu Q, Tang H, Mu Y, Pu Z, Li Y, Ma J, Gao Y, Jiang Q, Liu Y, Chen G, Wang J, Qi P, Habib A, Wei Y, Zheng Y, Lan X, Ma J. 2021. Genetic mapping and validation of loci for kernel-related traits in wheat (*Triticum aestivum* L.). *Frontiers in Plant Science*, **12**, 667493.
Ramya P, Chaubal A, Kulkarni K, Gupta L, Kadoo N, Dhaliwal H, Chhuneja P, Lagu M, Gupt V. 2010. QTL mapping of 1000-kernel weight, kernel length, and kernel width in bread wheat (*Triticum aestivum* L.). *Journal of Applied Genetics*, **51**, 421–429.
Shaw L M, Turner A S, Herry L, Griffiths S, Laurie D A. 2013. Mutant alleles of *Photoperiod-1* in wheat (*Triticum aestivum* L.) that confer a late flowering phenotype in long days. *PLoS ONE*, **8**, e79459.
Stein N, Herren G, Keller B. 2001. A new DNA extraction method for high-throughput marker analysis in a large-genome species such as *Triticum aestivum*. *Plant Breeding*, **120**, 354–356.
Sun C, Zhang F, Yan X, Zhang X, Dong Z, Cui D, Chen F. 2017. Genome-wide association study for 13 agronomic traits reveals distributiaon of superior alleles in bread wheat from the Yellow and Huai Valley of China. *Plant Biotechnology Journal*, **15**, 953–969.
Sun J, Sun Y, Ahmed R I, Ren A, Xie M. 2019. Research progress on plant RING-finger proteins. *Genes*, **10**, 973.
Wang J, Wang R, Mao X, Zhang J, Liu Y, Xie Q, Yang X, Chang X, Li C, Zhang X, Jing R. 2020. RING finger ubiquitin E3 ligase gene *TaSDIR1*-4A contributes to determination of grain size in common wheat. *Journal of Experimental Botany*, **71**, 5377–5388.
Xiao W, Hu S, Zou X, Cai R, Liao R, Lin X, Yao R, Guo X. 2021. Lectin receptor-like kinase *LecRK-VIII*. *2* is a missing link in MAPK signaling-mediated yield control. *Plant Physiology*, **187**, 303–320.
Xie X, Li S, Liu H, Xu Q, Tang H, Mu Y, Deng M, Jiang Q, Chen G, Qi P, Li W, Pu Z, Habib A, Wei Y, Zheng Y, Lan X, Ma J. 2022. Identification and validation of a major QTL for kernel length in bread wheat based on two F_3 biparental populations. *BMC Genomics*, **23**, 386.
Xin F, Zhu T, Wei S, Han Y, Zhao Y, Zhang D, Ma L, Ding Q. 2020. QTL mapping of kernel traits and validation of a major QTL for kernel length–width ratio using SNP and bulked segregant analysis in wheat. *Scientific Reports*, **10**, 25.
Yan P, Zhu Y, Wang Y, Ma F, Lan D, Niu F, Dong S, Zhang X, Hu J, Liu S, Guo T, Xin X, Zhang S, Yang J, Cao L, Luo X. 2022. A new RING finger protein, PLANT ARCHITECTURE and GRAIN NUMBER 1, affects plant architecture and grain yield in rice. *International Journal of Molecular Sciences*, **23**, 824.
You J, Liu H, Wang S, Luo W, Gou L, Tang H, Mu Y, Deng M, Jiang Q, Chen G, Qi P, Peng Y, Tang L, Habib A, Wei Y, Zheng Y, Lan X, Ma J. 2021. Spike density quantitative trait loci detection and analysis in tetraploid and hexaploid wheat recombinant inbred line populations. *Frontiers in Plant Science*, **12**, 796397.
Zhao C, Zhou J, Li C, You J, Liu Y, Tang H, Deng M, Xu Q, Zhang Y, Jiang Q, Chen G, Qi P, Jiang Y, Wang J, Li W, Pu Z, Chen G, Jiang Y, Zheng Z, Liu C, *et al.* 2023. A major QTL simultaneously increases the number of spikelets per spike and thousand-kernel weight in a wheat line. *Theoretical and Applied Genetics*, **136**, 213.
Zheng Y, Lan X, Wei Y, Zhou Y, Liu D, Yang J, Yan J. 2002. Analysis on agronomic character of new wheat variety Chuannong 16. *Journal of Sichuan Agricultural University*, **20**, 194–197. (in Chinese)
Zhou J, Li C, You J, Tang H, Mu Y, Jiang Q, Liu Y, Chen G, Wang J, Qi P, Ma J, Gao Y, Habib A, Wei Y, Zheng Y, Lan X, Ma J. 2021. Genetic identification and characterization of chromosomal regions for kernel length and width increase from tetraploid wheat. *BMC Genomics*, **22**, 706.
Zhu X, Rong W, Wang K, Guo W, Zhou M, Wu J, Ye X, Wei X, Zhang Z. 2022. Overexpression of *TaSTT3b-2B* improves resistance to sharp eyespot and increases grain weight in wheat. *Plant Biotechnology Journal*, **20**, 777–793.